Fragmented Cooper pair condensation in striped superconductors

Alexander Wietek[1, 2, *]

[1]*Center for Computational Quantum Physics, Flatiron Institute, 162 Fifth Avenue, New York, NY 10010, USA*
[2]*Max Planck Institute for the Physics of Complex Systems,*
Nöthnitzer Strasse 38, Dresden 01187, Germany
(Dated: October 19, 2022)

Condensation of bosons in Bose-Einstein condensates or Cooper pairs in superconductors refers to a macroscopic occupation of a few single- or two-particle states. A condensate is called "fragmented" if not a single, but multiple states are macroscopically occupied. While fragmentation is known to occur in particular Bose-Einstein condensates, we propose that fragmentation naturally takes place in striped superconductors. To this end, we investigate the nature of the superconducting ground state realized in the two-dimensional t-t'-J model. In the presence of charge density modulations, the condensate is shown to be fragmented and composed of partial condensates located on the stripes. The fragments of the condensates hybridize to form an extended macroscopic wave function across the system. The results are obtained from evaluating the singlet-pairing two-particle density matrix of the ground state on finite cylinders computed via the density matrix renormalization group (DMRG) method. Our results shed light on the intricate relation between stripe order and superconductivity in systems of strongly correlated electrons.

INTRODUCTION

Superconductivity constitutes one of the most fascinating ramifications of quantum mechanics in macroscopic condensed matter systems. A key role in our understanding of high-temperature superconductivity is attributed to the two-dimensional Hubbard model, or its strong coupling limit, the t-J model [1–3]. Early on it was realized, that the essential behavior of the copper-oxide superconductors might be captured by these basic models. Solving these models, however, has posed major difficulties which have fueled the development of sophisticated numerical and analytical methods over the last decades [4–6]. These efforts have led to considerable progress in recent years [5, 7–10]. The emergence of stripes in certain relevant regions of the phase diagram, first proposed by Hartree-Fock studies [11–14], has by now been firmly established by a broad range of numerical methods [15–20]. The more intricate question of whether superconductivity is realized at low temperature in these models is currently being tackled by various approaches [21]. This year, three density matrix renormalization group (DMRG) [22, 23] studies have reported robust d-wave superconductivity in particular regimes of the hole-doped t-t'-J model [24–26]. Refs. [24, 26] employed advanced large-scale DMRG simulations to achieve convergence towards power-law decay of superconducting pairing correlations, indicative of a quasi-1D descendant of a 2D superconductor. Ref. [25] applied pinning fields, to demonstrate strong d-wave pairing in an extended region of the phase diagram.

In this manuscript, we investigate the nature of the superconducting condensate in this model in further detail. We propose to study the eigenvalues and eigenvectors of a properly chosen two-particle density matrix, which describe the superconducting condensate fraction and the macroscopic condensate wave function. The method is applied to the superconducting ground state of the t-t'-J model obtained from DMRG on cylinders of width $W = 4$ and $W = 6$. We discover, that in the presence of stripes, not just one global superconducting condensate but multiple condensates are formed. Each partial condensate is found to be associated with a single charge stripe. The occurrence of multiple condensates, corresponding to multiple dominant eigenvalues of the two-body density matrix is called *fragmentation*. Fragmentation is known to occur in specific instances of Bose-Einstein condensates [27–30]. Examples include in weakly-interacting spinor condensates [31] and exciton condensates [32]. However, fragmentation has to the best of our knowledge not prominently been discussed in the context of high-temperature superconductivity. The method of studying eigenvalues and eigenvectors of a two-particle density matrix is applicable for any numerical method, but particularly well-suited for DMRG. We, therefore, suggest this approach as a reliable means of diagnosing superconductivity in correlated electron systems.

TWO-PARTICLE DENSITY MATRICES

The essential quantity to study condensation of Cooper pairs is the generic two-particle density matrix ρ_2 [33],

$$\rho_2(\boldsymbol{r}_i\sigma_i, \boldsymbol{r}_j\sigma_j | \boldsymbol{r}_k\sigma_k, \boldsymbol{r}_l\sigma_l) = \langle c^\dagger_{\boldsymbol{r}_i\sigma_i} c^\dagger_{\boldsymbol{r}_j\sigma_j} c_{\boldsymbol{r}_k\sigma_k} c_{\boldsymbol{r}_l\sigma_l} \rangle, \quad (1)$$

where $\sigma_i = \uparrow, \downarrow$ denotes the fermion spin and $c^\dagger_{\boldsymbol{r}_i\sigma_i}$ and $c_{\boldsymbol{r}_i\sigma_i}$ are fermion creation and annihilation operators at lattice positions $\boldsymbol{r}_i$. Since ρ_2 is Hermitian,

$$\rho_2(\boldsymbol{r}_i\sigma_i, \boldsymbol{r}_j\sigma_j | \boldsymbol{r}_k\sigma_k, \boldsymbol{r}_l\sigma_l) = \rho_2^*(\boldsymbol{r}_k\sigma_k, \boldsymbol{r}_l\sigma_l | \boldsymbol{r}_i\sigma_i, \boldsymbol{r}_j\sigma_j), \quad (2)$$

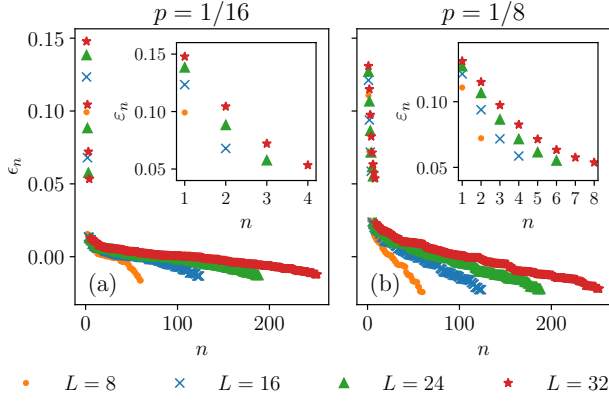FIG. 1. Spectrum ε_n of the singlet density matrix $\hat{\rho}_S$ of the ground state on the width $W = 4$ cylinder at $t' = 0.2$ and $J = 0.4$. We compare system lengths $L = 8, 16, 24, 32$ and show results for hole-doping $p = 1/16$ (a) and $p = 1/8$ (b). The number of dominant eigenvalues above the residual continuum exactly matches the number of stripes in the system. The insets zoom in on the largest eigenvalues. The condensate fractions ε_n increase with system size.

it can be diagonalized with real eigenvalues ε_n and eigenvectors χ_n,

$$\rho_2(\boldsymbol{r}_i\sigma_i, \boldsymbol{r}_j\sigma_j | \boldsymbol{r}_k\sigma_k, \boldsymbol{r}_l\sigma_l) = \sum_n \varepsilon_n \chi_n^*(\boldsymbol{r}_i\sigma_i, \boldsymbol{r}_j\sigma_j)\chi_n(\boldsymbol{r}_k\sigma_k, \boldsymbol{r}_l\sigma_l). \quad (3)$$

In analogy to Bose-Einstein condensation, Cooper pair condensation takes place whenever one or more eigenvalues are of order N, where N is the number of lattice sites. If exactly one eigenvalue is of order N the condensate is referred to as *simple*. If more than one eigenvalue is of order N, the condensate is called *fragmented* [33]. Dominant eigenvalues ε_i are referred to as the condensate fractions.

While the above definitions are rather generic in scope, we focus on more specific quantities to investigate singlet-pairing in two-dimensional lattice models. First, we define the singlet-pairing density matrix ρ_S as,

$$\rho_S(\boldsymbol{r}_i, \boldsymbol{r}_j | \boldsymbol{r}_k, \boldsymbol{r}_l) = \langle \Delta_{\boldsymbol{r}_i\boldsymbol{r}_j}^\dagger \Delta_{\boldsymbol{r}_k\boldsymbol{r}_l} \rangle, \quad (4)$$

where the singlet-pairing operators $\Delta_{\boldsymbol{r}_i\boldsymbol{r}_j}$ is given by

$$\Delta_{\boldsymbol{r}_i\boldsymbol{r}_j}^\dagger = \frac{1}{\sqrt{2}}\left(c_{\boldsymbol{r}_i\uparrow}^\dagger c_{\boldsymbol{r}_j\downarrow}^\dagger - c_{\boldsymbol{r}_i\downarrow}^\dagger c_{\boldsymbol{r}_j\uparrow}^\dagger\right). \quad (5)$$

To focus on two-dimensional lattice geometries, we consider a nearest-neighbor singlet density matrix,

$$\rho_S(\boldsymbol{r}_i, \alpha | \boldsymbol{r}_j, \beta) = \rho_S(\boldsymbol{r}_i, (\boldsymbol{r}_i + \alpha) | \boldsymbol{r}_j, (\boldsymbol{r}_j + \beta)), \quad (6)$$

where α (resp. β) denote the vectors connecting nearest-neighbors on the lattice, e.g. $\alpha = \hat{\boldsymbol{x}}, \hat{\boldsymbol{y}}$ in the case of a
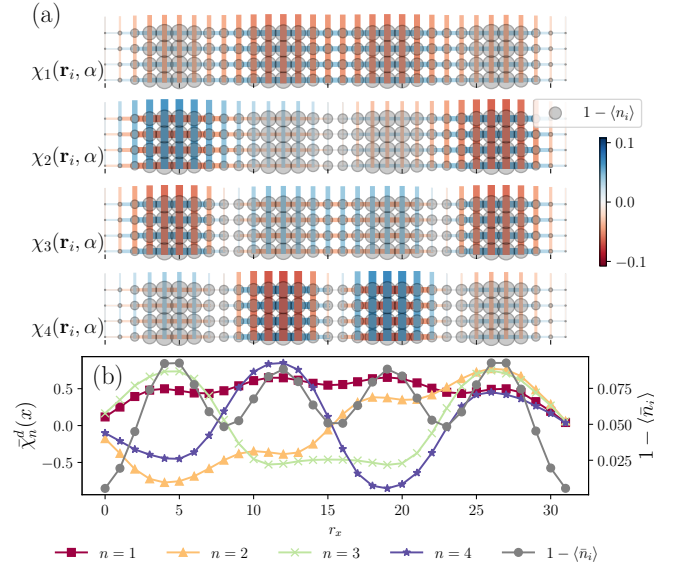

FIG. 2. (a) Condensate wave functions $\chi_n(\boldsymbol{r}_i, \alpha)$ for the dominant four eigenvalues of the two-body density matrix on a 32×4 cylinder at doping $p = 1/16$ and $t' = 0.2$. For $\alpha = \hat{\boldsymbol{x}}$ we show the value of $\chi_n(\boldsymbol{r}_i, \alpha)$ as the color and line width right to the site $\boldsymbol{r}_i$, for $\alpha = \hat{\boldsymbol{y}}$ it is shown on the link on top of site $\boldsymbol{r}_i$. Blue (red) indicates a positive (negative) value of $\chi_n(\boldsymbol{r}_i, \alpha)$. The hole-density $1 - \langle n_i \rangle$ is shown as the area of the gray circles. We observe uniform d-wave pattern, where vertical and horizontal bonds have opposite signs in the most dominant condensate wave function, while the other dominant condensates exhibit modulation of the d-wave orientation concomitant with the stripes. (b) Rung-averaged d-wave condensate wave function $\bar{\chi}_i^d$ and the rung-averaged hole-density $1 - \langle \bar{n}_i \rangle$.

square lattice. Again, this matrix can be decomposed into eigenvectors,

$$\rho_S(\boldsymbol{r}_i, \alpha | \boldsymbol{r}_j, \beta) = \sum_n \varepsilon_n \chi_n^*(\boldsymbol{r}_i, \alpha)\chi_n(\boldsymbol{r}_j, \beta). \quad (7)$$

The eigenvectors $\chi_n(\boldsymbol{r}_i, \alpha)$ are also referred to as *macroscopic wave functions*. They depend only on the position $\boldsymbol{r}_i$ and the direction of the nearest-neighbor α. In order to exclude local contributions from density and spin correlations, we consider the non-local singlet density matrix,

$$\hat{\rho}_S(\boldsymbol{r}_i, \alpha | \boldsymbol{r}_j, \beta) =$$
$$= \begin{cases} \rho_S(\boldsymbol{r}_i, \alpha | \boldsymbol{r}_j, \beta) & \text{if } \{\boldsymbol{r}_i, \boldsymbol{r}_i + \alpha\} \cap \{\boldsymbol{r}_j, \boldsymbol{r}_j + \beta\} = \emptyset \\ 0 & \text{else.} \end{cases} \quad (8)$$

We note, that with this choice, $\hat{\rho}_S$ is not necessarily positive definite. Thus, eigenvalues of $\hat{\rho}_S$ can in general be positive or negative.

SUPERCONDUCTIVITY IN THE t-t'-J MODEL

We now investigate the properties of the condensate fractions ε_n and macroscopic wave functions $\chi_n(\boldsymbol{r}_i, \alpha)$ of (non-)superconducting stripe states emerging in a simple model system of strongly interacting electrons. To this end, we study the two-dimensional t-t'-J model,

$$
\begin{aligned}
H = & - t \sum_{\langle ij \rangle, \sigma} c_{i\sigma}^\dagger c_{j\sigma} + \text{H.c.} - t' \sum_{\langle\langle ij \rangle\rangle, \sigma} c_{i\sigma}^\dagger c_{j\sigma} + \text{H.c.} \\
& + J \sum_{\langle ij \rangle} \left(\vec{S}_i \cdot \vec{S}_j - \frac{1}{4} n_i n_j \right),
\end{aligned} \tag{9}
$$

on a square lattice ($c_{i\sigma}^\dagger, c_{i\sigma} = c_{\boldsymbol{r}_i\sigma}^\dagger, c_{\boldsymbol{r}_i\sigma}$). Here, $\vec{S}_i = (S_i^x, S_i^y, S_i^z)$ are the spin operators, and $n_i = \sum_\sigma c_{i\sigma}^\dagger c_{i\sigma}$ denotes the local density operator. The sums over $\langle i, j \rangle$ are over nearest-neighbor sites and $\langle\langle i, j \rangle\rangle$ denotes a sum over next-nearest neighbors. The Hilbert space is constrained to prohibit doubly occupied configurations. In the following, we set $t = 1$ and $J = 0.4$ which is the same set of parameters chosen in Ref. [25]. Our model slightly differs from the model studied in Ref. [24], where also next-nearest neighbor Heisenberg interactions have been included. While superconductivity of the ground states in particular parameter regimes has already been established [24–26, 34], a detailed investigation of two-body density matrices has not previously been performed.

We apply the DMRG method to study the system on cylindrical geometries with open boundary conditions along the long x-direction and periodic boundary conditions along the short y-direction. The length in the x-direction is denoted by L, and the width in the y-direction by W. Previous DMRG studies of Eq. (9) have achieved ground state simulations of widths of $W = 8$ [25]. In this manuscript, we focus on the particular cases of $W = 4, 6$, which do not require large computational resources to achieve convergence for the ground state. Thus, our computations are less challenging as $W = 8$ and, therefore, more easily reproducible. The results in this manuscript have been attained with bond dimensions up to $D = 2000$.

We first focus on the case of width $W = 4$ cylinders and choose $t' = 0.2$ with hole-dopings $p = 1/16$ and $p = 1/8$. A previous DMRG study of this model on the width $W = 4$ has established an approximate phase diagram [34]. For $t' = 0.2$ with hole-dopings $p = 1/16$ and $p = 1/8$ the system has been found to exhibit a Luther-Emery liquid (the LE2 phase in Ref. [34]) in this regime, with half-filled charge stripes and pronounced algebraic superconducting correlations.

We computed the singlet density matrix $\hat{\rho}_S(\boldsymbol{r}_i, \alpha | \boldsymbol{r}_j, \beta)$ by measuring the respective pairing correlations of the ground state obtained via DMRG. The eigenvalues of the singlet density matrix are for cylinder lengths $L = 8, 16, 24, 32$ in Fig. 1. The key observation is that only few
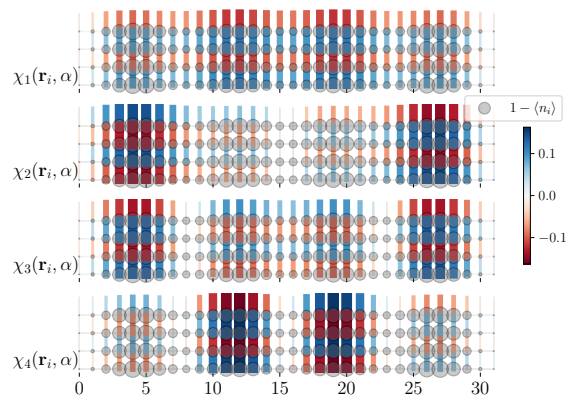

FIG. 3. Condensate wave functions $\chi_n(\boldsymbol{r}_i, \alpha)$ for the dominant four eigenvalues of $\hat{\rho}_S$ on a 32×4 cylinder at doping $p = 1/16$ and $t' = 0$. The hole-density $1 - \langle n_i \rangle$ is shown as the area of the gray circles.

dominant eigenvalues are separated from a continuum of minor eigenvalues. At hole-doping $p = 1/16$ shown in (a), the system realizes one stripe for $L = 8$, two stripes for $L = 16$, three stripes for $L = 24$, and four stripes for $L = 32$, as can be seen for $L = 32$ in Fig. 2. Correspondingly, we observe exactly one dominant eigenvalue for $L = 8$, two dominant eigenvalues for $L = 16$, three dominant eigenvalues for $L = 24$, and four dominant eigenvalues for $L = 32$. Hence, the number of dominant eigenvalues exactly matches the number of stripes in the system. The same observation is made at hole-doping $p = 1/8$, where twice as many stripes are observed alongside twice as many dominant eigenvalues. These eigenvalues are interpreted as superconducting condensate fractions. The insets show a zoom on the dominant eigenvalues ε_n. In all cases, the condensate fraction increases monotonously with system size.

The structure of the four dominant macroscopic wave functions $\chi_n(\boldsymbol{r}_i, \alpha)$ on the $W = 4$ cylinder at $p = 1/16$ and $t' = 0.2$ is shown in in Fig. 2(a). The wave functions $\chi_n(\boldsymbol{r}_i, \alpha)$ depend both on the position $\boldsymbol{r}_i$ as well as the nearest-neighbor direction α. When $\alpha = \hat{\boldsymbol{x}}$ we show the value of $\chi_n(\boldsymbol{r}_i, \alpha)$ to the lattice edge right of site $\boldsymbol{r}_i$, if $\alpha = \hat{\boldsymbol{y}}$ it is shown on the edge on top of site $\boldsymbol{r}_i$. We also show the local density of holes, $1 - \langle n_i \rangle$ superimposed. The most dominant condensate wave function shown on top exhibits clearly extended uniform d-wave pattern, where horizontal and vertical bonds have opposite signs. The other two dominant modes exhibit a uniform d-wave pattern on a single stripe, while the orientation and amplitude modulates between different stripes. A possible interpretation would be that uniform condensates form along the stripes of the system, which hybridize by tunneling through a barrier of higher electron density. Hence, the "fragments" of the condensate are individual condensates living on the stripes. To
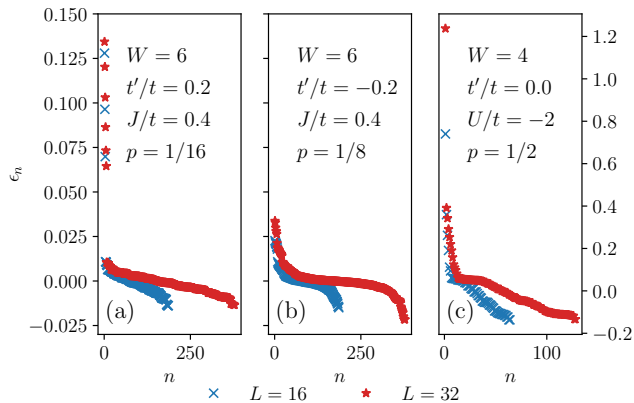
FIG. 4. Spectrum ε_n of $\hat{\rho}_S$ on the $W = 6$ cylinder for (a) the d-wave superconducting state at $t' = 0.2$, $p = 1/16$ and (b) a non-superconducting stripe state at $t' = -0.2$, $p = 1/8$. No dominant eigenvalues are observed in the non-superconducting case in (b). (c) Spectrum of $\rho_{\rm loc}$ (Eq. (11), diagonal elements have been set to zero) for the s-wave superconducting state realized in the attractive Hubbard model on a $W = 4$ cylinder for $U/t = -2$, $p = 1/2$, and $t'/t = 0$. Only one dominant eigenvalue is observed for this uniform condensate.

demonstrate the relation between the condensates and the stripes more clearly, we show the rung-averaged d-wave condensate wave function,

$$\bar{\chi}_n^d(r_x) = \sum_{y=1}^{W} \chi_n\left((r_x, r_y), \hat{\boldsymbol{x}}\right) - \chi_n\left((r_x, r_y), \hat{\boldsymbol{y}}\right), \quad (10)$$

in Fig. 2(b) alongside the rung-averaged hole density $1 - \langle \bar{n}_i \rangle$, where $\bar{n}_i = \frac{1}{W} \sum_{j=1}^{W} n_{(x_i, y_j)}$.

We observe that the modulations of $\bar{\chi}_n^d(r_x)$ correspond exactly to the modulations in the charge density.

Next, we show that the fragmentation of the condensate is not just a particular feature of the LE2 phase on the $W = 4$ cylinder but is more generic. We consider a different superconducting phase, which is stabilized on the $W = 4$ cylinder, the plaquette-pairing phase at $t' = 0$ and $p = 1/16$ [35], referred to as LE1 phase in Ref. [34]. The plaquette-pairing phase is a peculiarity of the width $W = 4$ cylinder, where pairing is formed along the four-site plaquettes of the cylinder and is different from the typical d-wave pairing state. The spectrum ε_n of $\hat{\rho}_S$ closely resembles the case $t' = 0.2$, and the exact same number of dominant eigenvalues is observed. The condensate wave functions are shown in Fig. 3(a). We clearly observe a plaquette pairing pattern, where the sign of $\chi_n(\boldsymbol{r}, \alpha)$ alternates in the y-direction, while pairing along the $\hat{\boldsymbol{x}}$ direction is suppressed. Similar to the d-wave condensates in Fig. 2, $\chi_n(\boldsymbol{r}, \alpha)$ is modulated by the stripes of the system.

The physics of the width $W = 6$ cylinder is different from the $W = 4$ cylinder in certain aspects. As estab-
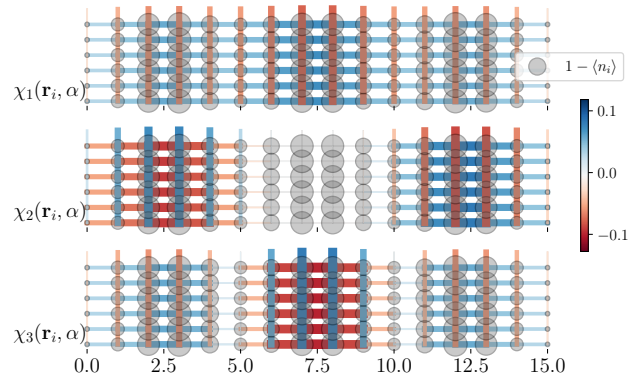

FIG. 5. Condensate wave functions $\chi_n(\boldsymbol{r}_i, \alpha)$ for the dominant three eigenvalues of $\hat{\rho}_S$ on a 16×6 cylinder at doping $p = 1/16$ and $t' = 0.2$. The hole-density $1 - \langle n_i \rangle$ is shown as the area of the gray circles.

lished in Refs. [24–26], for $t' < 0$ no superconductivity is observed and a charge density wave is stabilized. However, at small to intermediate doping and finite $t' > 0$, a superconducting phase has been found. In Fig. 4 we show the spectrum of $\hat{\rho}_S$ in both the superconducting phase at $t' = 0.2$ and $p = 1/16$ in panel (a) as well as the non-superconducting stripe phase at $t' = -0.2$ and $p = 1/8$ in panel (b). Only in the superconducting phase do we observe dominant eigenvalues, whose number again exactly matches the number of charge stripes. Therefore, the observation of dominant eigenvalues ε_n is clearly associated with the superconductivity and not just the stripe order of the system. The associated macroscopic wave functions to the three dominant eigenvalues for $t' = 0.2$ and $p = 1/16$ on the 16×6 cylinder are shown in Fig. 5. Again, we observe a uniform d-wave pattern in the leading eigenvalue, which is modulated in the other two eigenvalues. To assess the stability of the fragmentation in the two-dimensional limit we compare the gap δ between the smallest dominant eigenvalue and the largest non-dominant eigenvalue between the $W = 4$ and $W = 6$ cylinders. We computed $\delta = 0.041$ on the 32×4 cylinder and $\delta = 0.054$ on the 32×6 cylinder. Hence, the gap is increasing with cylinder width, which is an indication of the stability of the condensate in the two-dimensional limit.

We also consider the case of uniform s-wave superconductivity without the formation charge density wave. Such a state is realized in the attractive (negative-U) Hubbard model on the square lattice [36, 37]. Due to a difference in the pairing mechanism we consider the site-local pairing density matrix,

$$\rho_{\rm loc}(\boldsymbol{r}_i|\boldsymbol{r}_j) = \langle \Delta_{\boldsymbol{r}_i}^{\dagger} \Delta_{\boldsymbol{r}_j} \rangle \quad \text{where} \quad \Delta_{\rm r_i}^{\dagger} = c_{\rm r_i\uparrow}^{\dagger} c_{\rm r_i\downarrow}^{\dagger}. \quad (11)$$

Fig. 4(c) shows that a single dominant eigenvalue is formed at $U/t = -2$ and $t'/t = 0$ on the W=4 cylin-
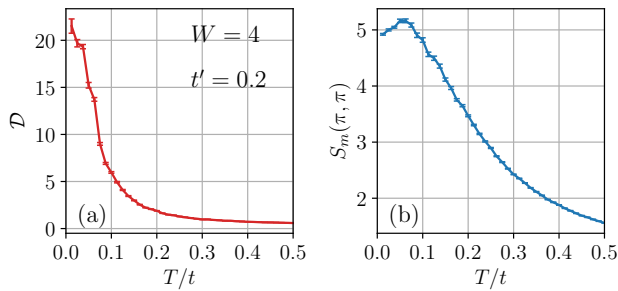
FIG. 6. Temperature dependence of the d-wave pairing susceptibility $\mathcal{D}$ (a) and the antiferromagnetic spin structure factor $S_m(\pi, \pi)$ (b) for $t - t' - J$ model on the 32×4 cylinder at $p = 1/16$ and $t' = 0.2$. Strong pairing correlations develop below a temperature $T/t \approx 0.05$, which suppresses antiferromagnetism.

der at quarter filling, i.e. $p = 1/2$ increasing with system size.

Finally, we investigate how the fragmented condensate can emerge from a "normal" state. Therefore, we study the temperature dependence of the d-wave pairing susceptibility,

$$\mathcal{D} = \sum_{\alpha, \beta} (-1)^{\alpha \cdot \beta + 1} \sum_{\mathbf{r}_i, \mathbf{r}_j} \hat{\rho}_S(\mathbf{r}_i, \alpha | \mathbf{r}_j, \beta), \qquad (12)$$

and the magnetic structure factor $S_m(\mathbf{q})$ at the antiferromagnetic ordering vector $\mathbf{q} = (\pi, \pi)$ using the METTS method with maximal bond dimension $D = 2000$ [20, 38]. We observe that strong pairing correlations develop below a temperature of $T/t \approx 0.05$. Antiferromagnetic correlations develop at a higher temperature but are finally suppressed by pairing correlations.

DISCUSSION AND CONCLUSION

Our results suggest a simple physical picture of the interplay of stripe order and superconductivity. Individual superconducting condensates are formed on the stripes of the system and hole-pairs can tunnel through a barrier given by the maxima in the electron density. The superconducting stripes could thus be regarded as an emergent array of Josephson junctions. While we found the most dominant macroscopic wave function to be a uniform superposition of the condensate fragments, it is an important open question under which circumstances different modes, e.g. a π-phase shift Josephson junction, could be realized as the dominant contribution. Moreover, the smallest dominant eigenvectors shown in Fig. 2 ($n = 4$) and Fig. 5 ($n = 3$) are pair-density waves [39], where the condensate wave function is modulated from stripe to stripe. Such states have previously been suggested for the t-t'-J model from variational Monte Carlo

simulations [40]. Interestingly, recent experiments on $\mathrm{La_{2-x}Ba_x CuO_4}$ have highlighted the possibility of having pair correlations within stripes without coherence between the stripes [41, 42]. This observation could indeed be explained by the fragmentation of the superconducting state by stripes, a fundamental mechanism we have now revealed in the t-t'-J model.

* awietek@pks.mpg.de

[1] P. W. Anderson, The Resonating Valence Bond State in $\mathrm{La_2CuO_4}$ and Superconductivity, Science **235**, 1196 (1987).

[2] F. C. Zhang and T. M. Rice, Effective Hamiltonian for the superconducting Cu oxides, Phys. Rev. B **37**, 3759 (1988).

[3] V. J. Emery and G. Reiter, Mechanism for high-temperature superconductivity, Phys. Rev. B **38**, 4547 (1988).

[4] M. Imada, A. Fujimori, and Y. Tokura, Metal-insulator transitions, Rev. Mod. Phys. **70**, 1039 (1998).

[5] M. Qin, T. Schäfer, S. Andergassen, P. Corboz, and E. Gull, The hubbard model: A computational perspective (2021), arXiv:2104.00064.

[6] D. P. Arovas, E. Berg, S. A. Kivelson, and S. Raghu, The hubbard model, Annu. Rev. Condens. Matter Phys. **13**, 239 (2022).

[7] A. M. S. Tremblay, B. Kyung, and D. Sénéchal, Pseudogap and high-temperature superconductivity from weak to strong coupling. Towards a quantitative theory (Review Article), Low Temperature Physics **32**, 424 (2006).

[8] T. A. Maier, M. Jarrell, T. Pruschke, and M. Hettler, Quantum cluster theories, Rev. Mod. Phys. **77**, 1027 (2005).

[9] F. Šimkovic IV, R. Rossi, and M. Ferrero, The weak, the strong and the long correlation regimes of the two-dimensional hubbard model at finite temperature (2021), arXiv:2110.05863.

[10] T. Schäfer, N. Wentzell, F. Šimkovic, Y.-Y. He, C. Hille, M. Klett, C. J. Eckhardt, B. Arzhang, V. Harkov, F. m. c.-M. Le Régent, A. Kirsch, Y. Wang, A. J. Kim, E. Kozik, E. A. Stepanov, A. Kauch, S. Andergassen, P. Hansmann, D. Rohe, Y. M. Vilk, J. P. F. LeBlanc, S. Zhang, A.-M. S. Tremblay, M. Ferrero, O. Parcollet, and A. Georges, Tracking the footprints of spin fluctuations: A multimethod, multimessenger study of the two-dimensional hubbard model, Phys. Rev. X **11**, 011058 (2021).

[11] J. Zaanen and O. Gunnarsson, Charged magnetic domain lines and the magnetism of high-T_c oxides, Phys. Rev. B

40, 7391 (1989).

[12] D. Poilblanc and T. M. Rice, Charged solitons in the hartree-fock approximation to the large-u hubbard model, Phys. Rev. B **39**, 9749 (1989).

[13] K. Machida, Magnetism in La_2CuO_4 based compounds, Physica C: Superconductivity **158**, 192 (1989).

[14] M. Kato, K. Machida, H. Nakanishi, and M. Fujita, Soliton lattice modulation of incommensurate spin density wave in two dimensional hubbard model -a mean field study-, J. Phys. Soc. Japan **59**, 1047 (1990).

[15] G. B. Martins, C. Gazza, J. C. Xavier, A. Feiguin, and E. Dagotto, Doped stripes in models for the cuprates emerging from the one-hole properties of the insulator, Phys. Rev. Lett. **84**, 5844 (2000).

[16] J. P. F. LeBlanc, A. E. Antipov, F. Becca, I. W. Bulik, G. K.-L. Chan, C.-M. Chung, Y. Deng, M. Ferrero, T. M. Henderson, C. A. Jiménez-Hoyos, E. Kozik, X.-W. Liu, A. J. Millis, N. V. Prokof'ev, M. Qin, G. E. Scuseria, H. Shi, B. V. Svistunov, L. F. Tocchio, I. S. Tupitsyn, S. R. White, S. Zhang, B.-X. Zheng, Z. Zhu, and E. Gull (Simons Collaboration on the Many-Electron Problem), Solutions of the two-dimensional hubbard model: Benchmarks and results from a wide range of numerical algorithms, Phys. Rev. X **5**, 041041 (2015).

[17] B.-X. Zheng, C.-M. Chung, P. Corboz, G. Ehlers, M.-P. Qin, R. M. Noack, H. Shi, S. R. White, S. Zhang, and G. K.-L. Chan, Stripe order in the underdoped region of the two-dimensional Hubbard model, Science **358**, 1155 (2017).

[18] E. W. Huang, C. B. Mendl, S. Liu, S. Johnston, H.-C. Jiang, B. Moritz, and T. P. Devereaux, Numerical evidence of fluctuating stripes in the normal state of high-T_c cuprate superconductors, Science **358**, 1161 (2017).

[19] E. W. Huang, C. B. Mendl, H.-C. Jiang, B. Moritz, and T. P. Devereaux, Stripe order from the perspective of the Hubbard model, npj Quantum Materials **3**, 22 (2018).

[20] A. Wietek, Y.-Y. He, S. R. White, A. Georges, and E. M. Stoudenmire, Stripes, antiferromagnetism, and the pseudogap in the doped hubbard model at finite temperature, Phys. Rev. X **11**, 031007 (2021).

[21] M. Qin, C.-M. Chung, H. Shi, E. Vitali, C. Hubig, U. Schollwöck, S. R. White, and S. Zhang (Simons Collaboration on the Many-Electron Problem), Absence of superconductivity in the pure two-dimensional hubbard model, Phys. Rev. X **10**, 031016 (2020).

[22] S. R. White, Density matrix formulation for quantum renormalization groups, Phys. Rev. Lett. **69**, 2863 (1992).

[23] S. R. White, Density-matrix algorithms for quantum renormalization groups, Phys. Rev. B **48**, 10345 (1993).

[24] S. Gong, W. Zhu, and D. N. Sheng, Robust d-wave superconductivity in the square-lattice $t-j$ model, Phys. Rev. Lett. **127**, 097003 (2021).

[25] S. Jiang, D. J. Scalapino, and S. R. White, Ground-state phase diagram of the t-t'-j model, Proc. Natl. Acad. Sci. U.S.A. **118**, 10.1073/pnas.2109978118 (2021).

[26] H.-C. Jiang and S. A. Kivelson, High temperature superconductivity in a lightly doped quantum spin liquid, Phys. Rev. Lett. **127**, 097002 (2021).

[27] R. W. Spekkens and J. E. Sipe, Spatial fragmentation of a bose-einstein condensate in a double-well potential, Phys. Rev. A **59**, 3868 (1999).

[28] T.-L. Ho and S. K. Yip, Fragmented and single condensate ground states of spin-1 bose gas, Phys. Rev. Lett. **84**, 4031 (2000).

[29] E. J. Mueller, T.-L. Ho, M. Ueda, and G. Baym, Fragmentation of bose-einstein condensates, Phys. Rev. A **74**, 033612 (2006).

[30] M.-K. Kang and U. R. Fischer, Revealing single-trap condensate fragmentation by measuring density-density correlations after time of flight, Phys. Rev. Lett. **113**, 140404 (2014).

[31] B. Evrard, A. Qu, J. Dalibard, and F. Gerbier, Observation of fragmentation of a spinor bose-einstein condensate, Science **373**, 1340 (2021).

[32] M. Combescot, R. Combescot, M. Alloing, and F. m. c. Dubin, Effects of fermion exchange on the polarization of exciton condensates, Phys. Rev. Lett. **114**, 090401 (2015).

[33] A. J. Leggett, *Quantum Liquids* (Oxford University Press, Great Clarendon Street Oxford, 2006).

[34] Y.-F. Jiang, J. Zaanen, T. P. Devereaux, and H.-C. Jiang, Ground state phase diagram of the doped hubbard model on the four-leg cylinder, Phys. Rev. Research **2**, 033073 (2020).

[35] C.-M. Chung, M. Qin, S. Zhang, U. Schollwöck, and S. R. White (The Simons Collaboration on the Many-Electron Problem), Plaquette versus ordinary d-wave pairing in the t'-hubbard model on a width-4 cylinder, Phys. Rev. B **102**, 041106 (2020).

[36] R. T. Scalettar, E. Y. Loh, J. E. Gubernatis, A. Moreo, S. R. White, D. J. Scalapino, R. L. Sugar, and E. Dagotto, Phase diagram of the two-dimensional negative-u hubbard model, Phys. Rev. Lett. **62**, 1407 (1989).

[37] T. Paiva, R. R. dos Santos, R. T. Scalettar, and P. J. H. Denteneer, Critical temperature for the two-dimensional attractive hubbard model, Phys. Rev. B **69**, 184501 (2004).

[38] A. Wietek, R. Rossi, F. Šimkovic, M. Klett, P. Hansmann, M. Ferrero, E. M. Stoudenmire, T. Schäfer, and A. Georges, Mott insulating states with competing orders in the triangular lattice hubbard model, Phys. Rev. X **11**, 041013 (2021).

[39] D. F. Agterberg, J. S. Davis, S. D. Edkins, E. Fradkin, D. J. Van Harlingen, S. A. Kivelson, P. A. Lee, L. Radzihovsky, J. M. Tranquada, and Y. Wang, The physics of pair-density waves: Cuprate superconductors and beyond, Annu. Rev. Condens. Matter Phys. **11**, 231 (2020).

[40] A. Himeda, T. Kato, and M. Ogata, Stripe states with spatially oscillating d-wave superconductivity in the two-dimensional $t-t'-J$ model, Phys. Rev. Lett. **88**, 117001 (2002).

[41] Y. Li, J. Terzic, P. G. Baity, D. Popović, G. D. Gu, Q. Li, A. M. Tsvelik, and J. M. Tranquada, Tuning from failed superconductor to failed insulator with magnetic field, Sci. Adv. **5**, eaav7686 (2019).

[42] J. Wårdh, M. Granath, J. Wu, A. T. Bollinger, X. He, and I. Božović, Colossal transverse magnetoresistance due to nematic superconducting phase fluctuations in a copper oxide (2022), arXiv:2203.06769.

[43] M. Fishman, S. R. White, and E. M. Stoudenmire, The ITensor software library for tensor network calculations (2020), arXiv:2007.14822.